Egypt. J. Chem. **Vol. 68**, No. 4, pp. 405 - 416 (2025)

Egyptian Journal of Chemistry

http://ejchem.journals.ekb.eg/

Removal Of BTX From Aqueous Solutions by Adsorption Using PDMS Foam

Lila Alatawi[a,b], Abdul Halim Abdullah[a,c,*], Siti Nurul Ain Md. Jamil[a,d], Robiah Yunus[f]

[a]*Department of Chemistry, Faculty of Science, Universiti Putra Malaysia, 43400 UPM Serdang, Selangor, Malaysia*

[b]*Department of Chemistry, Faculty of Science, University of Tabuk, Tabuk, Saudi Arabia*

[c]*Institute of Nanoscience and Nanotechnology, Universiti Putra Malaysia, 43400 UPM Serdang, Selangor, Malaysia*

[d]*Centre of Foundation Studies for Agricultural Science, University Putra Malaysia, 43400 UPM Serdang, Selangor Malaysia.*

[f]*Department of Chemical and Environmental Engineering, Faculty of Engineering, Universiti Putra Malaysia, 43400 UPM Serdang, Selangor, Malaysia*

Abstract

Due to untreated wastewater disposal from a growing population and industry, biological and chemical pollutants have accumulated in the environment. Benzene, toluene, and xylene (BTX) are among the most frequently encountered contaminants in industrial wastewater. Due to their toxic and carcinogenic nature, BTX-containing industrial wastewater requires proper treatment prior to discharge to open water. This study examined the monocomponent adsorption of BTX from an aqueous solution using polydimethylsiloxane (PDMS) foam. Adsorption performance was optimised under various experimental conditions, including the effects of contact time, adsorption dosage, and initial concentration. The adsorption capacity of PDMS foam followed the order X > T > B, and the equilibrium of adsorption was reached in 6 h. The adsorption isotherms were analysed using the Langmuir, Freundlich, and Temkin models to evaluate their suitability for fitting the experimental data. The kinetics of the process were assessed employing both the pseudo-first-order and pseudo-second-order models. The adsorption data exhibited a good fit with Freundlich isotherms and a pseudo-second-order kinetic model. Based on experimental findings, PDMS foam shows great promise as an effective adsorbent for removing BTX from water.

Keywords: PDMS foam; gas foaming process; BTX removal; adsorption isotherm; adsorption kinetic.

Introduction

Access to freshwater is essential for the sustenance of humans and wildlife. Despite the fact that approximately 97.5% of the Earth's total water resources are comprised of seawater, there remains a significant shortage of freshwater for human use. This shortage causes a significant challenge to communities worldwide. Access to safe drinking water is essential for promoting overall health and well-being. Individuals face heightened risks of waterborne diseases and other health complications without adequate access to clean water. As a result of the rapidly growing population and industrial activity, biological and chemical pollutants have accumulated in the environment due to the disposal of untreated wastewater [1,2]. The pharmaceutical industry, along with sectors including detergents, plastics, inks, paints, and adhesives, significantly contributes to the contaminant concentrations in wastewater. The disposable wastes of these industries contain petrochemical materials such as BTX, which refers to benzene, toluene, and xylene as they are used as starting materials. [3–5] Even at low concentrations, BTX is detrimental to human health on account of its exceptionally high toxicity and carcinogenic characteristics. Additionally, leukaemia, fatal deficiencies of the nervous system, and irritation of the skin, eyes, and mucous membranes may result from BTX exposure [3,6–9]. Thus, removing such harmful pollutants from wastewater is a critical global concern.

The two main techniques applied to control BTX are destruction and recovery. Catalytic oxidation, thermal oxidation, and biodegradation are examples of destruction techniques, while absorption, adsorption, and membrane separation are examples of recovery techniques [10–16]. The sorption process has been demonstrated to be both technically and economically effective for removing organic compounds from water.

*Corresponding author e-mail: lialatawi@ut.edu.sa; (Lila Alatawi).
Receive Date: 26 June 2024, Revise Date: 08 August 2024, Accept Date: 18 August 2024
DOI: 10.21608/ejchem.2024.299520.9906

Various sorbents, such as commercial organoclay [10], activated sludge [17], activated carbon [18], and periodic mesoporous organosilica [19], have been used in the removal of BTX from wastewater. However, there are some difficulties in using these sorbents, such as complex preparation, low working capacity, and low recyclability. Moreover, removing sorbents from the solution requires pre-treatment methods like centrifugation or filtration, which limit large-scale application. Thus, there is a strict necessity to develop cost-effective, non-toxic, and eco-friendly adsorbents.

Recently, there has been a lot of interest in porous polymeric materials like polydimethylsiloxane (PDMS) due to their excellent characteristics. PDMS foam has many applications in different fields because of its hydrophobicity, simple fabrication, low cost, remarkable reusability, large surface area, high flexibility, elasticity, and thermal stability. Some of its applications include sensors, microfluidics, adsorbents, absorbents, and oil/water separation [20–23]. PDMS foams have been manufactured using various methods, including porogen leaching [21,24–34], gaseous blowing agents [1,35,36], and emulsion techniques [37–43]. However, the porogen leaching approach requires toxic solvents and a long processing time. On the other hand, the surfactants used in the emulsion method must be eliminated because they affect the quality of the foam.

Additionally, studies that employed the gas blowing approach to generate PDMS foam either coupled it with other techniques or added more hazardous substances, making the process more complicated, time-consuming, and non-eco-friendly.

This work introduces a fast, easy, and effective method for preparing PDMS foam via gas foaming. There is minimal work available in the literature on the formation of PDMS foam using this method. Most reported works employed HCl and HNO_3 as catalysts. For the first time, this work explored using green materials, namely acetic acid as a catalyst and NaHCO3 as a blowing agent, to produce PDMS foam. This process has minimal environmental impact, as no waste materials result from the preparation process. It is hypothesised that the foam has excellent selectivity, ensuring it only adsorbs the desired contaminants, leaving the surrounding water or environment unaffected, making it suitable for large-scale applications.

Materials and Methods

Materials

A Sylgard-184 kit from Dow Corning is provided in two components: Sylgard-184 A (base) and Sylgard-184 B (curing agent). Acetic acid and sodium bicarbonate were purchased from R&M Chemicals. Benzene with 99.5% purity, toluene with 99% purity, and mixtures of isomers of xylene with 98.5% purity were obtained from System Chemicals.

Preparation of PDMS foams

The PDMS foam was prepared based on prior work [44]. First, the PDMS base and curing agent were combined in a 10:1 mass ratio, thoroughly mixing until a homogeneous prepolymer liquid formed. Then, sodium bicarbonate was added at 5% by weight and acetic acid at 10% by weight to the PDMS prepolymer. The mixture was stirred manually until it was uniform and the sodium bicarbonate was fully dispersed. The mixture was placed in a preheated oven at 100 °C, curing for one hour. After curing, the mould was removed from the oven, allowed to cool to room temperature, and then the formed PDMS foam was extracted. The foams were washed with water to remove any residual chemicals and allowed to air dry completely before further use.

Characterisation

The foam morphology was examined using a field emission scanning electron microscope (FE-SEM JEOL JSM-7600F, Tokyo, Japan). The obtained SEM images were analysed using Fiji/ImageJ software, V 1.8.0. The FTIR spectra were acquired on the Thermo Fisher Scientific Nicolet iS10 spectrometer, USA, in the region of 400–4000 cm^{-1}.

Adsorption experiments

B, T, and X adsorption from aqueous solutions onto PDMS foams in mono-component systems was carried out via batch adsorption in gas-tight glass vials. Each vial contained the adsorbent (0.2 g) and the adsorbate solution (40 mL) with different concentrations at room temperature. Each experiment was carried out in triplicate. A blank experiment was also performed in the absence of the adsorbent to evaluate and determine any potential loss of BTX due to volatilisation. The influence of key adsorption parameters (the amount of adsorbent used, the time of contact, and the initial concentration) on the uptake behaviour of BTX on PDMS foam was explored.

The impact of contact time was examined at varying intervals within the range of 15–360 minutes. To assess the influence of adsorbent dosage, the amount of PDMS foam was varied from 0.04 to 1.4 g/40 mL on 100 ppm of B, T, and X solutions at 25 °C for six hours. The impact of the initial BTX concentration on the uptake process was examined by altering the concentrations within the range of 50 to 500 mg/L for B and T and from 30 to 150 mg/L for X. The total time needed to reach equilibrium for adsorption was six hours.

A Lambda 35 UV-Vis spectrophotometer (PerkinElmer Life) was used to determine the adsorbate concentration at the respective maximum wavelengths (λ_{max}) of 254 nm, 261 nm, and 264 nm for B, T, and X.

The adsorption capacity of BTX by PDMS foam was obtained by Equations (1)

$$\boldsymbol{q_e}\textbf{(mg/g)} = \frac{(C_0 - C_e)V}{m} \qquad (1)$$

The removal efficiency of BTX by PDMS foam was obtained by Equations (2)

$$\%\boldsymbol{R} = \frac{C_0 - C_e}{C_0} \times \mathbf{100} \qquad (2)$$

where q_e (mg/g) is the adsorption capacity at equilibrium, C_0 (mg/L) and C_e (mg/L) represent the initial and equilibrium concentrations of BTX, respectively, m (g) is the mass of PDMS foam, and V (L) represents the volume of the BTX solution.

Adsorption isotherm

The adsorption isotherm describes the equilibrium between the concentration of an adsorbate in a solution and the amount of that adsorbate adsorbed onto a solid surface. The adsorption isotherm shape reflects the solute's adsorption behaviour and the adsorbent's surface properties. The most commonly used adsorption isotherms are the Langmuir, Freundlich, and Temkin models, extensively studied and applied in various areas, such as environmental research, biotechnology, and materials science [45,46]. For the study of the adsorption isotherms, three different models were utilised in their linear form:

the Langmuir model (Equations 3)

$$\frac{C_e}{q_e} = \frac{1}{q_{max}K_L} + \frac{C_e}{q_{max}} \qquad (3)$$

the Freundlich model (Equations 4)

$$\ln(q_e) = \ln(K_F) + \frac{1}{n}\ln(C_e) \qquad (4)$$

Temkin isotherm model (Equations 5)

$$q_e = B_1\ln(K_T) + B_1\ln(C_e) \qquad (5)$$

Where: q_{max} (mg/g): maximum adsorption capacity of BTX, K_L, K_F and K_T: constants of Langmuir, Freundlich, and Temkin, respectively. Also, n and B_1: constants related to the intensity of the adsorption and adsorption heat, in that order [47–49].

Kinetic Studies

Adsorption kinetics are mathematical expressions that explain the duration needed for the adsorption process to achieve equilibrium. Kinetic models can be used to make predictions about the behaviour of chemical reactions under different conditions. They are an essential tool for understanding the mechanisms of chemical reactions and also provide data for the design and modelling of this process [50–52]. Two distinct kinetic models were applied to analyse the kinetic batch experimental data:

The pseudo-first-order kinetic model (Equations 6)

$$\log(q_e - q_t) = \log(q_e) - K_1\frac{t}{2.303} \qquad (6)$$

The pseudo-second-order kinetic model (Equations 7)

$$\frac{t}{q_t} = \frac{1}{K_2(q_e)^2} + \frac{t}{q_e} \qquad (7)$$

Where: q_e (mg/g): adsorption quantity at equilibrium, q_t (mg/g): adsorption amount at any time t (min), K_1 (min^{-1}) and K_2 (g/mg.min): rate constants of the pseudo-first-order and pseudo-second-order, respectively [48,53].

Results and Discuss

Preparation of PDMS foams

The PDMS foam was produced through the gas-blowing process. Heating the mixture in the oven led to the crosslinking of the polymer (Figure 1). In addition, the decomposition of $NaHCO_3$ and the reaction between acetic acid and $NaHCO_3$ took place, releasing the CO_2 gas responsible for the porous structures generated in the PDMS foam.

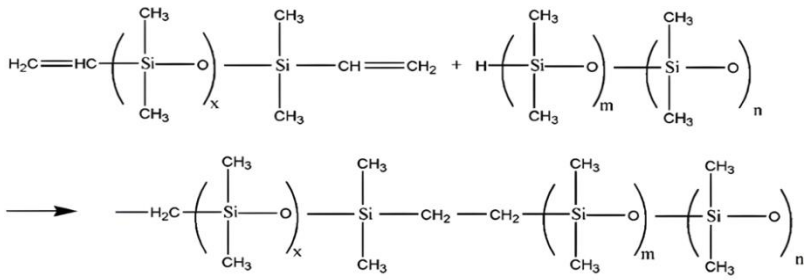

Fig. 1: Crosslinking reaction of PDMS foams [54]

Characterisation

Morphology

The morphology of the PDMS foam, synthesised using 2:1 $NaHCO_3$:acetic acid ratios and cured at 100°C, exhibits homogeneous and uniform porosity (Figures 2A and B). The figures show connected micropores with diameters less than 100 µm and spherical interconnected macropores with sizes between 100 µm and 1000 µm. The pore homogeneity may be

explained by the simultaneous emission of CO_2 throughout the curing stage, resulting in the simultaneous generation of cells and making the pores in the foam uniform. Figure 2 (C) shows the foam pore-size distributions determined based on the FESEM image. Most of the pores are less than 600 µm in diameter, with a peak between 100 µm and 200 µm.

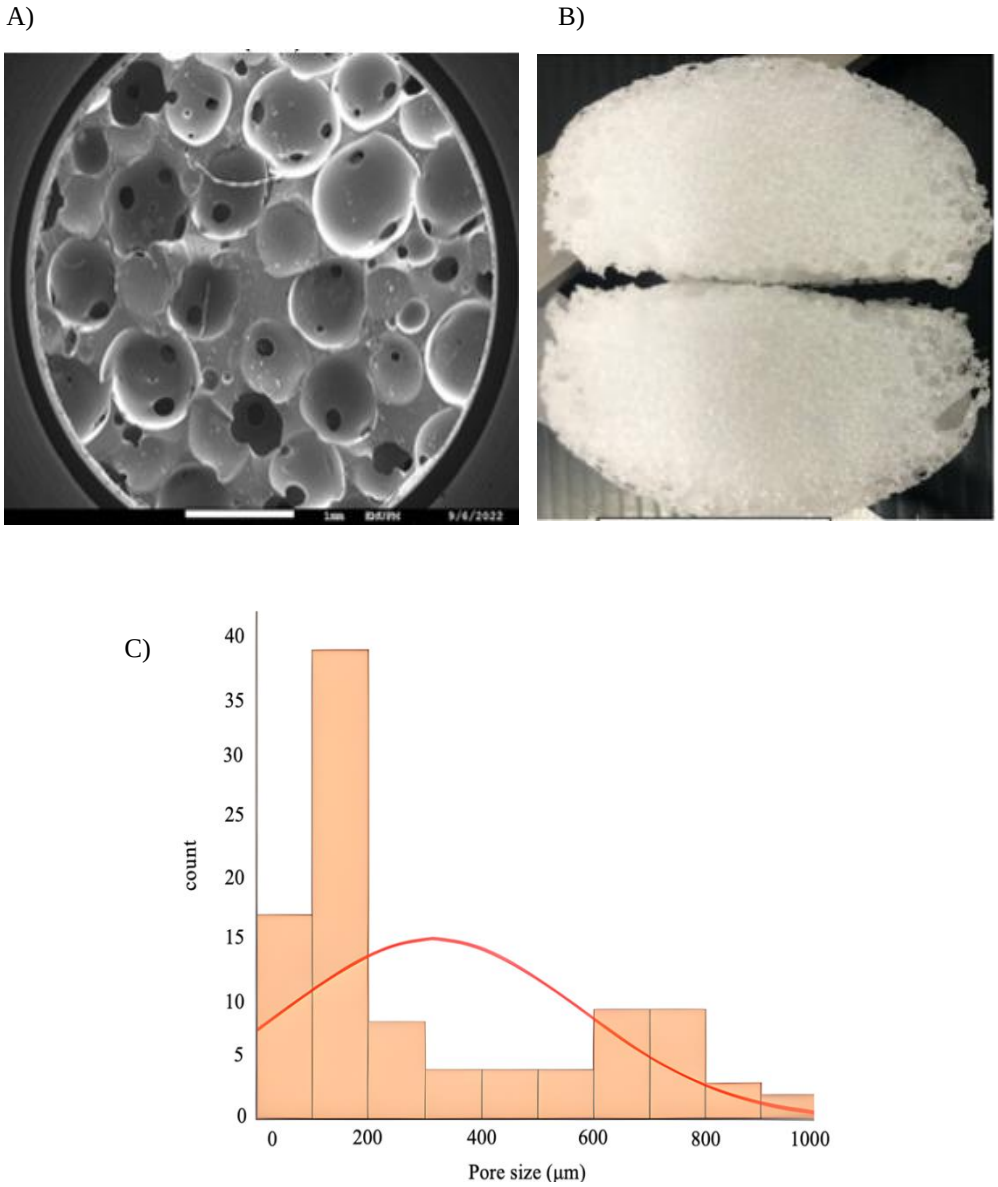

Fig. 2 A) FESEM photograph of PDMS foams. B) Photograph of of PDMS foam. C) pore size distribution of PDMS foam.

Fourier transform infrared spectroscopy (FTIR)

The functional groups present in the foam were determined through analysis of the FTIR spectra of the PDMS foam, as depicted in Figure 3. The significant peak at 1009 cm^{-1}, which is the distinctive peak of the backbone of PDMS foam, is attributed to the stretching of Si-O-Si bonds. The main absorption bands in the FTIR spectra of PDMS foam are illustrated in Table 1 [27,54,58].

Table 1 Main absorption bands in the FTIR spectra of PDMS foam

Wavenumber (cm^{-1})	Assignment
787	Si-CH_3 stretching
843	-CH_3 rock
1009	Si-O-Si stretching
1257	C-H bending.
1412	C-H bending.
2962	C-H stretching

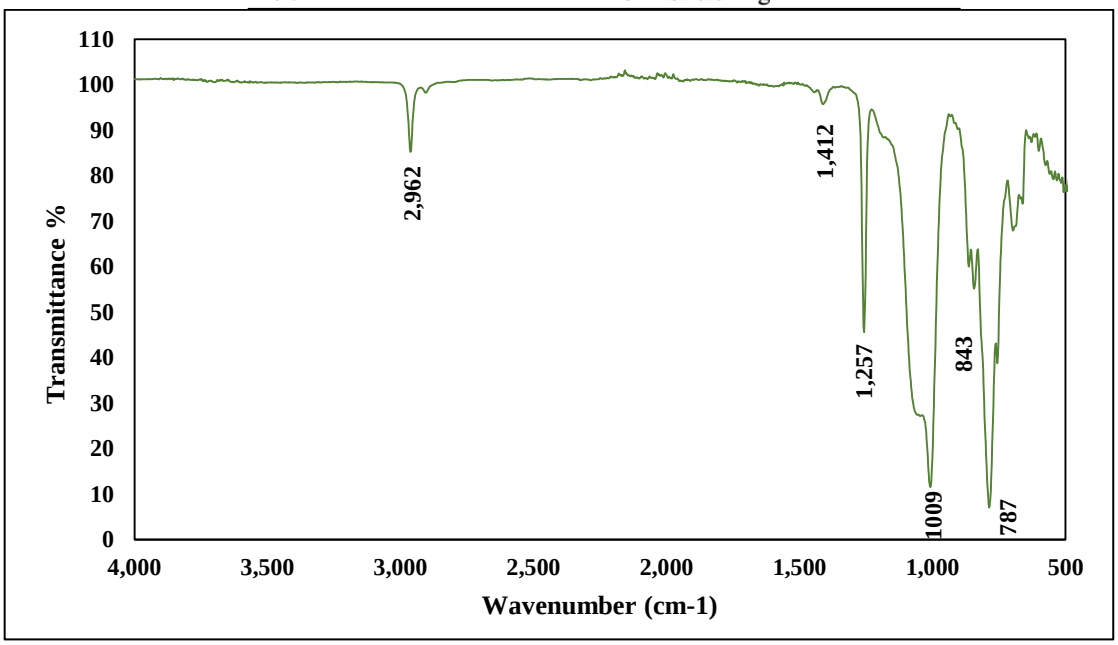

Fig. 3 FTIR spectra of PDMS foam

Adsorption study

Effect of Contact Time

The influence of contact time on the adsorption of 100 mg/L of B, T, and X is illustrated in Figure 4. The adsorption capacities rapidly increased for the first 120 minutes due to the availability of vacant active sites, but increased slightly with increasing contact time as occupying the remaining adsorption sites became difficult due to repulsive forces between the adsorbate molecules adsorbed on the PDMS foam surface and those left in solution. After six hours, no significant changes in adsorption capacity indicated that the adsorption equilibrium was reached. The adsorption rate was in the order of X > T > B. This behaviour is attributed to several factors, namely solubility, the number of substituents, and the molecular size of BTX. The water solubility of BTX is in the order of X < T < B. As the least soluble compound, X is less surrounded by water molecules, making it easier to interact with the PDMS foam, leading to a higher adsorption capacity. The number of CH_3 substituents also increases from zero (B) to two (X), which in turn increases the molecular size of the compound (X > T > B). The larger the size of the molecules, the higher the interaction between the molecules and the PDMS foam, reflecting the adsorption rate order [59–63]. The increase of the methyl group (an electron-donating group) on the aromatic ring increases the electron density of the benzene ring, thus increasing the affinity of BTX to PDMS foam in the order X > T > B [59–63].

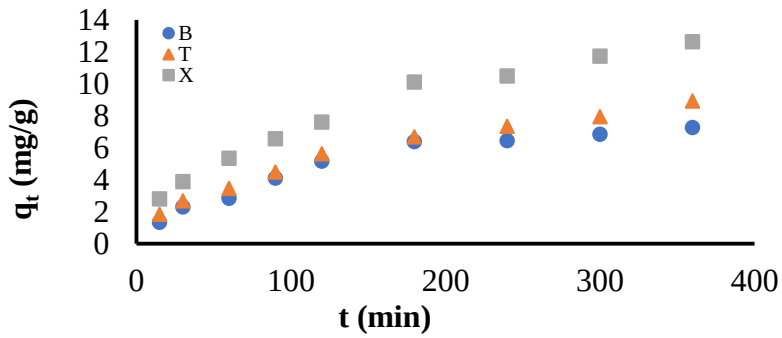

Fig. 4 The effect of contact time on the adsorption of 100 mg/L of B, T, and X by PDMS foam

Effect of Adsorbent Dosage

The dependence of B, T, and X adsorption capacity and adsorption efficiency on the PDMS foam dosage while maintaining other process variables constant is demonstrated in Figure 5, Figure 6, and Figure 7, respectively. The increase in the PDMS dosage led to a decrease in adsorption capacity, which was associated with the unsaturation of available active sites due to an increase in adsorbent dose at the same volume and concentration of BTX solution. However, the removal efficiency increases as the PDMS dosage increases. The increase in removal efficiency is associated with the increased availability of active sites. The intersection point in the graph is considered the optimum dose because it represents a balance between B removal efficiency and adsorption capacity. Hence, 0.2 g was selected as the optimum dose and was applied in further analyses.

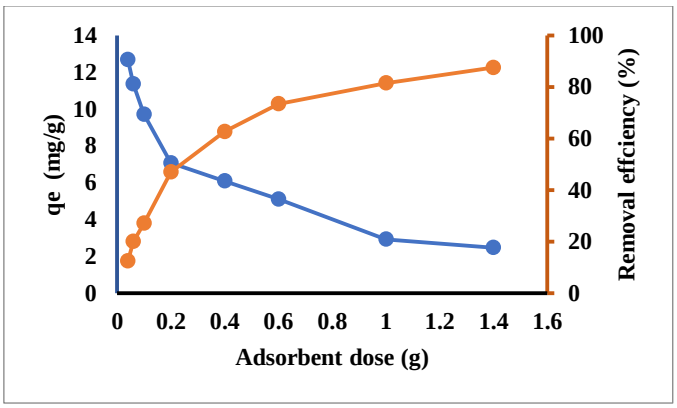

Fig. 5 Effect of adsorbent dose on the adsorption capacity of PDMS foam for the removal of B

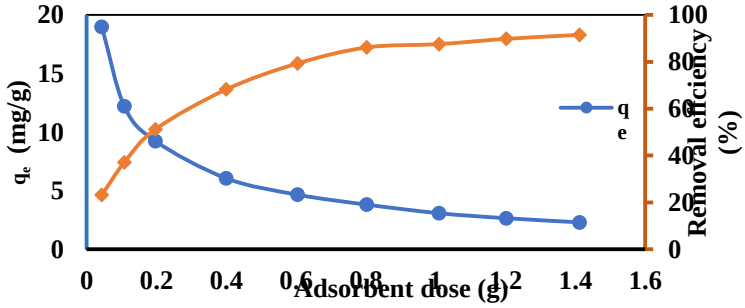

Fig. 6 Effect of adsorbent dose on the adsorption capacity of PDMS foam for the removal of T

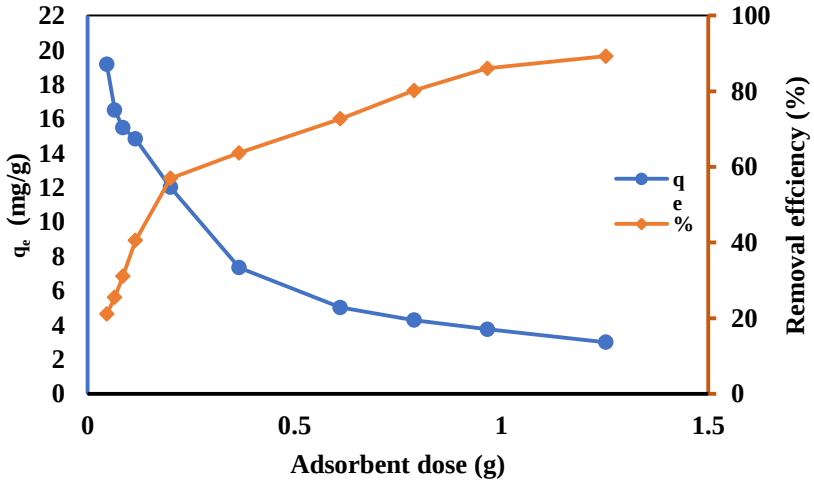

Fig. 7 Effect of adsorbent dose on the adsorption capacity of PDMS foam for the removal of X

Effect of Initial BTX Concentration

Figure 8 presents the impact of the initial BTX concentration on the adsorption capacity of PDMS foam. The q_e values increased with increasing adsorbate concentrations. Typically, this behaviour can be attributed to the increased driving force induced by the concentration gradient. As the BTX molecules in the solution increase, more BTX molecules surround the active sites of the PDMS foam, thus increasing the probability of BTX-PDMS interaction.

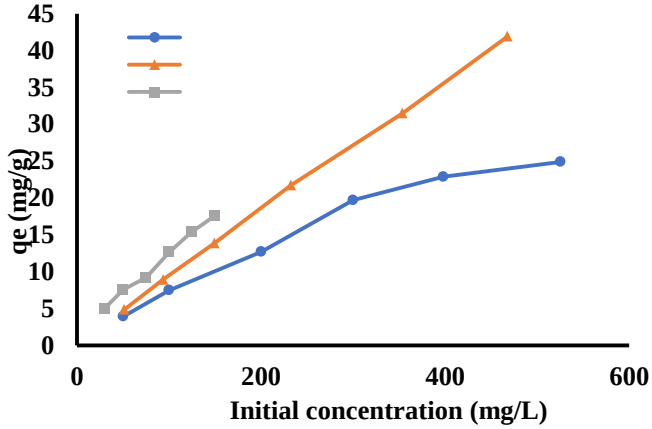

Fig. 8 Effect of initial BTX concentrate on the adsorption capacity of PDMS foam

Adsorption Isotherms Models

Three isotherm models, namely, Langmuir, Freundlich, and Temkin isotherms, were examined to interpret an interaction of BTX with the PDMS foam. Figure 9 displays the adsorption isotherms, while Table 2 provides the related adsorption parameters. Based on the correlation coefficient R^2 values, the Freundlich model exhibited a better fit to the experimental data, meaning that the adsorption of BTX onto PDMS foam occurred at heterogeneous surfaces through a multilayer sorption system involving physical forces. The value of the parameter n in the Freundlich model indicates the favorability of the adsorption. Adsorption is favourable if the values of n are higher than unity. Therefore, BTX is favourably adsorbed by the PDMS foam, and their interaction is strong. The findings are compatible with other research studies [53,64]. The maximum adsorption capacity of several adsorbents for BTX is illustrated in Table 3.

Table 2 Adsorption parameters calculated from Langmuir, Freundlich, and Temkin isotherm models

	Parameter	**B**	**T**	**X**
Langmuir	q_{max} (mg/g)	46.948	243.902	23.529
	K_L (L/mg) x 10^3	3.02471	0.76756	35.76538
	R^2	0.9435	0.8839	0.8348
Freundlich	q_{max} (mg/g)	37.682	75.102	26.688
	$q_{(exp)}$ (mg/g)	25.605	45.460	17.593
	n	1.0972	1.0814	2.0032
	K_F mg/g(L/mg)$^{1/n}$	0.2603	0.2398	2.1878
	R^2	0.9939	0.9978	0.9967
Temkin	B_1 (J/mol)	8.665	13.279	4.762
	K_T (L/g)	0.043	16.576	2.282
	R^2	0.9639	0.8677	0.8730

Table 3 The maximum adsorption capacity of various adsorbents for BTX

Adsorbent	Maximum adsorption capacity, q_{max} (mg/g)			References
	B	T	X	
Thermally modified lignite	2.719	3.161	3.716	[53]
Zeolite Na-P1	0.032	0.0343	0.035	[65]
Smectite organoclay	0.52	0.69	0.75	[49]
Commercial Organoclay	0.938	2.765	14.865	[10]
Periodic mesoporous organosilica	0.6803	0.6207	0.6601	[19]
CNT sponge	0.13	2.45	14.31	[66]
PDMS foam	25.605	45.460	17.593	The present work

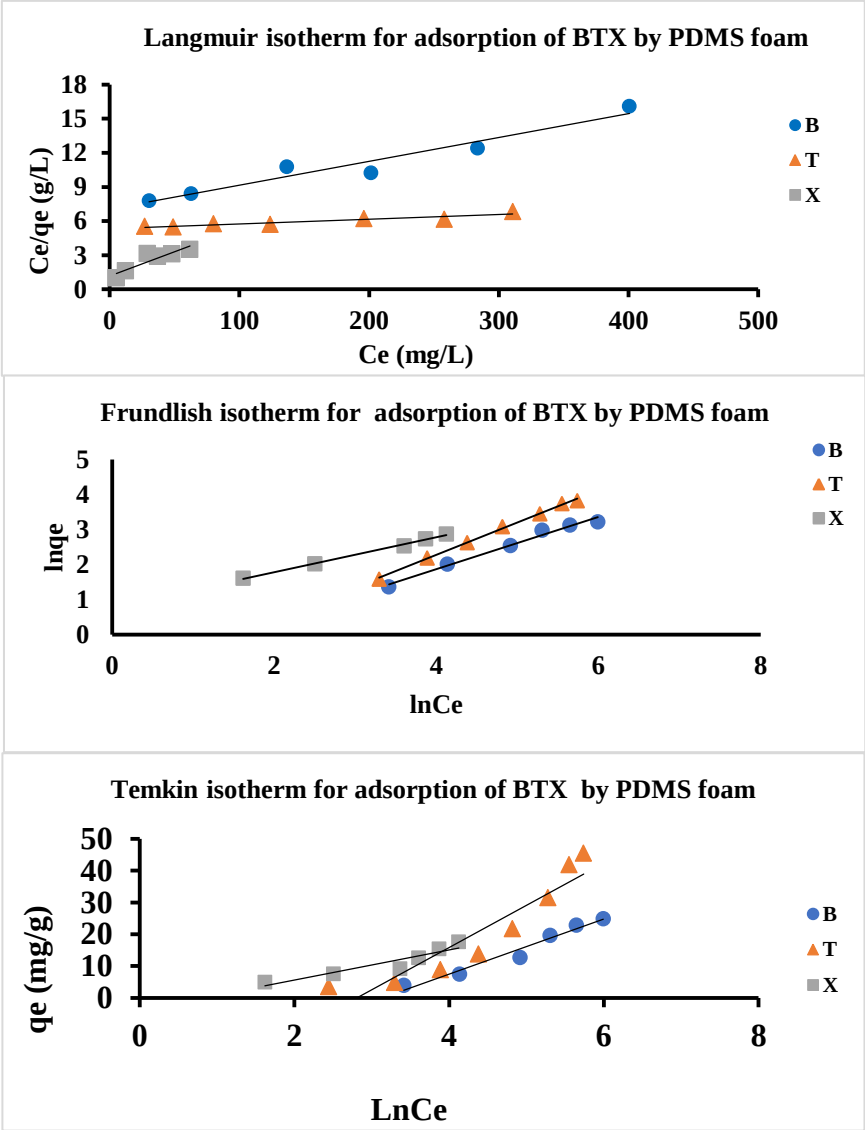

Fig. 9 Isotherm models for adsorption of BTX by PDMS foam **Kinetic Studies**

Figure 10 represents the linearised graph of a pseudo-second-order kinetic model for BTX. The parameters of the pseudosecond-order kinetic models for BTX are shown in Table 4. The correlation coefficient R^2 values of pseudosecond-order are much closer to unity. Furthermore, the theoretical values $q_{e(cal)}$ agree well with the corresponding experimental values $q_{e(exp)}$. Hence, the adsorption of BTX on PDMS foam is better described by the pseudo-second-order model. The findings are consistent with other research studies [64,65,67,68].

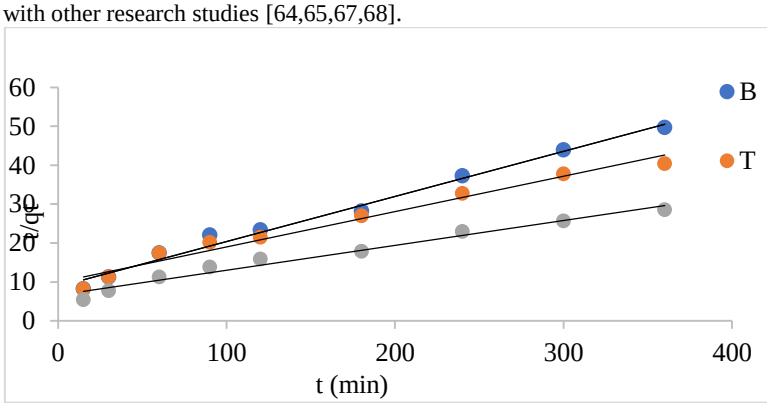

Fig. 10 Pseudo-second-order kinetic model for adsorption of BTX by PDMS foam

Table 4 Pseudo-second-order kinetic model parameters for the adsorption of BTX onto PDMS foam

Adsorbate	Initial concentration C_0 (mg/L)	$q_{e\,(exp)}$ (mg/g)	$q_{e\,(cal)}$ (mg/g)	K_2 (g/mg.h)	Rate (mg/g.h)	R^2
B	100	7.25	8.63	0.001521	0.1133	0.9874
T	100	8.92	11.03	0.000827	0.1006	0.9734
X	100	12.62	15.63	0.000619	0.1512	0.9751

Adsorption mechanism

The mechanism responsible for the adsorption of BTX on PDMS foam can be identified as the CH –π interaction, which arises mainly from charge transfer between the PDMS methyl groups and the π- electrons of BTX (Figure 11). Methyl groups are electron-donating, meaning they can increase the electron density of the aromatic ring. The increased electron density in the aromatic ring can enhance the CH-π interaction. In this interaction, the hydrogen atoms from CH groups on the PDMS foam can be attracted to the π electron cloud of the aromatic ring. The higher electron density in the aromatic ring makes it more attractive to the hydrogen atoms, strengthening the CH-π interaction. In BTX compounds, X has two methyl groups, T has one, and B has none, resulting in X having the strongest CH-π interaction with PDMS foam, followed by T and then B. Another potential interaction can be related to the hydrophobic nature of the PDMS foam and BTX. BTX are nonpolar substances and thus are considered hydrophobic molecules [59,60,62]. PDMS foam, composed mainly of repeating dimethylsiloxane units, is hydrophobic due to its surface's abundance of methyl groups. Being of similar properties, the affinity of BTX towards the hydrophobic surface of PDMS foam resulted in a higher BTX-PDMS interaction and, thus, a higher adsorption capacity.

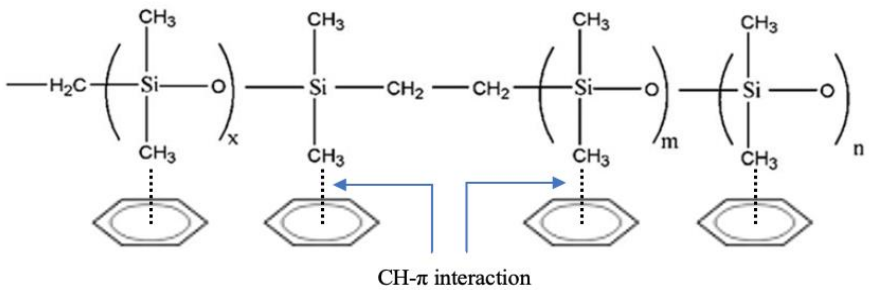

Fig 11: CH-π interaction between a benzene molecule and PDMS foam

Conclusions

This paper investigated the adsorption of BTX onto PDMS foam from aqueous solutions. After six hours, adsorption equilibrium was achieved. The adsorption capacity increases in the order X > T > B. Due to the increase of the methyl group on the aromatic ring, the electron density increased, reinforcing the CH –π interaction between BTX and PDMS foam. The Freundlich model was found to exhibit a better fit to the experimental data, meaning that the adsorption of BTX onto PDMS foam occurred at heterogeneous surfaces through a multilayer sorption system involving physical forces. The kinetics results revealed that the adsorption of BTX onto PDMS foam was best represented by the pseudo-second-order model. PDMS foam may constitute an efficient and environmentally friendly adsorbent for BTX removal.

References

1. Wang, H.; Zhang, R.; Yuan, D.; Xu, S.; Wang, L. Gas Foaming Guided Fabrication of 3D Porous Plasmonic Nanoplatform with Broadband Absorption, Tunable Shape, Excellent Stability, and High Photothermal Efficiency for Solar Water Purification. *Adv Funct Mater* **2020**, *30*, 1–8, doi:10.1002/adfm.202003995.
2. Sajid, M.; Nazal, M.K.; Ihsanullah; Baig, N.; Osman, A.M. Removal of Heavy Metals and Organic Pollutants from Water Using Dendritic Polymers Based Adsorbents: A Critical Review. *Sep Purif Technol* **2018**, *191*, 400–423, doi:10.1016/j.seppur.2017.09.011.
3. Tursi, A.; Chidichimo, F.; Bagetta, R.; Beneduci, A. BTX Removal from Open Aqueous Systems by Modified Cellulose Fibers and Evaluation of Competitive Evaporation Kinetics. *Water (Switzerland)* **2020**, *12*, 1–20, doi:10.3390/w12113154.
4. Fayemiwo, O.M.; Daramola, M.O.; Moothi, K. Btex Compounds in Water – Future Trends and Directions for Water Treatment. *Water SA* **2017**, *43*, 602–613, doi:10.4314/wsa.v43i4.08.
5. Zuiderveen, E.A.R.; Caldeira, C.; Vries, T.; Schenk, N.J.; Huijbregts, M.A.J.; Sala, S.; Hanssen, S. V.; van Zelm, R. Evaluating the Environmental Sustainability of Alternative Ways to Produce Benzene, Toluene, and Xylene. *ACS Sustain Chem Eng* **2024**, *12*, 5092–5104, doi:10.1021/acssuschemeng.3c06996.
6. Kuppusamy, S.; Maddela, N.R.; Megharaj, M.; Venkateswarlu, K. *Total Petroleum Hydrocarbons: Environmental Fate, Toxicity, and Remediation*; Total Petroleum Hydrocarbons, 2020; ISBN 9783030240356.

7. Wu, M.; Zhao, Z.; Cai, G.; Wang, C.; Cheng, G.; Wang, X. Adsorption Behaviour and Mechanism of Benzene, Toluene and m-Xylene (BTX) Solution onto Kaolinite: Experimental and Molecular Dynamics Simulation Studies. *Sep Purif Technol* **2022**, *291*, doi:10.1016/j.seppur.2022.120940.
8. Abdel-Aziz, M.A.; Younis, S.A.; Moustafa, Y.M.; Khalil, M.M.H. Synthesis of Recyclable Carbon/Lignin Biocomposite Sorbent for in-Situ Uptake of BTX Contaminants from Wastewater. *J Environ Manage* **2019**, *233*, 459–470, doi:10.1016/j.jenvman.2018.12.044.
9. Maswanganyi, C.; Tshilongo, J.; Mkhohlakali, A.; Martin, L. Investigation of BTX Concentrations and Effects of Meteorological Parameters in the Steelpoort Area of Limpopo Province, South Africa. *Atmosphere (Basel)* **2024**, *15*, doi:10.3390/atmos15050552.
10. Lima, L.F.; De Andrade, J.R.; Da Silva, M.G.C.; Vieira, M.G.A. Fixed Bed Adsorption of Benzene, Toluene, and Xylene (BTX) Contaminants from Monocomponent and Multicomponent Solutions Using a Commercial Organoclay. *Ind Eng Chem Res* **2017**, *56*, 6326–6336, doi:10.1021/acs.iecr.7b00173.
11. Hackbarth, F. V.; Vilar, V.J.P.; De Souza, G.B.; De Souza, S.M.A.G.U.; De Souza, A.A.U. Benzene, Toluene and o-Xylene (BTX) Removal from Aqueous Solutions through Adsorptive Processes. *Adsorption* **2014**, *20*, 577–590, doi:10.1007/s10450-014-9602-3.
12. Nourmoradi, H.; Nikaeen, M.; Khiadani, H.H. Removal of Benzene, Toluene, Ethylbenzene and Xylene (BTEX) from Aqueous Solutions by Montmorillonite Modified with Nonionic Surfactant: Equilibrium, Kinetic and Thermodynamic Study. *Chemical Engineering Journal* **2012**, *191*, 341–348, doi:10.1016/j.cej.2012.03.029.
13. Yuan, J.; Li, G.; Liu, X.; Yang, Y.; Yu, F.; Cao, J.; Fei, Z.; Ma, J.; Nazeeruddin, M.K.; Dyson, P.J. Catalytic Oxidation of BTX (Benzene, Toluene, and Xylene) Using Metal Oxide Perovskites. *Adv Funct Mater* 2024.
14. Aydin, D.C.; Faber, S.C.; Attiani, V.; Eskes, J.; Aldas-Vargas, A.; Grotenhuis, T.; Rijnaarts, H. Indene, Indane and Naphthalene in a Mixture with BTEX Affect Aerobic Compound Biodegradation Kinetics and Indigenous Microbial Community Development. *Chemosphere* **2023**, *340*, doi:10.1016/j.chemosphere.2023.139761.
15. Ghanbarnezhad, M.; Parvareh, A.; Keshavarz Moraveji, M.; Jorfi, S. Iranian Journal of Chemical Engineering Synthesize and Application of the Fe3O4/MW-CNT Composite in the Photo-Catalyst Assisted Electrochemical Oxidation of BTX Compounds From Wastewater. *Iranian Journal of Chemical Engineering* **2023**, *20*, 51–66, doi:10.22034/ijche.2023.394803.1489.
16. Almuhtaseb, R.M.; Bhagyaraj, S.; Krupa, I. A Concise Review on BTEX Remediation from Aqueous Solutions by Adsorption. *Emergent Mater* 2024, *7*, 695–719.
17. Ramteke, L.P.; Gogate, P.R. Removal of Benzene, Toluene and Xylene (BTX) from Wastewater Using Immobilized Modified Prepared Activated Sludge (MPAS). *Journal of Chemical Technology and Biotechnology* **2016**, *91*, 456–466, doi:10.1002/jctb.4599.
18. Saha, D.; Mirando, N.; Levchenko, A. Liquid and Vapor Phase Adsorption of BTX in Lignin Derived Activated Carbon: Equilibrium and Kinetics Study. *J Clean Prod* **2018**, *182*, 372–378, doi:10.1016/j.jclepro.2018.02.076.
19. Moura, C.P.; Vidal, C.B.; Barros, A.L.; Costa, L.S.; Vasconcellos, L.C.G.; Dias, F.S.; Nascimento, R.F. Adsorption of BTX (Benzene, Toluene, o-Xylene, and p-Xylene) from Aqueous Solutions by Modified Periodic Mesoporous Organosilica. *J Colloid Interface Sci* **2011**, *363*, 626–634, doi:10.1016/j.jcis.2011.07.054.
20. Michel, T.R.; Capasso, M.J.; Cavusoglu, M.E.; Decker, J.; Zeppilli, D.; Zhu, C.; Bakrania, S.; Kadlowec, J.A.; Xue, W. Evaluation of Porous Polydimethylsiloxane/Carbon Nanotubes (PDMS/CNTs) Nanocomposites as Piezoresistive Sensor Materials. *Microsystem Technologies* **2020**, *26*, 1101–1112, doi:10.1007/s00542-019-04636-4.
21. Zhu, D.; Handschuh-Wang, S.; Zhou, X. *Recent Progress in Fabrication and Application of Polydimethylsiloxane Sponges*; Journal of Materials Chemistry A, 2017; Vol. 5; ISBN 8675526536627.
22. Zhao, X.; Li, L.; Li, B.; Zhang, J.; Wang, A. Durable Superhydrophobic/Superoleophilic PDMS Sponges and Their Applications in Selective Oil Absorption and in Plugging Oil Leakages. *J Mater Chem A Mater* **2014**, *2*, 18281–18287, doi:10.1039/c4ta04406a.
23. Aslan, Y.; McGleish, O.; Reboud, J.; Cooper, J.M. Alignment-Free Construction of Double Emulsion Droplet Generation Devices Incorporating Surface Wettability Contrast. *Lab Chip* **2023**, *23*, 5173–5179, doi:10.1039/d3lc00584d.
24. Liu, L.; Chen, J.; Zhang, W.; Fan, M.; Gong, Z.; Zhang, J. Graphene Oxide/Polydimethylsiloxane Composite Sponge for Removing Pb(Ii) from Water. *RSC Adv* **2020**, *10*, 22492–22499, doi:10.1039/d0ra03057k.
25. Rinaldi, A.; Tamburrano, A.; Fortunato, M.; Sarto, M.S. A Flexible and Highly Sensitive Pressure Sensor Based on a PDMS Foam Coated with Graphene Nanoplatelets. *Sensors* **2016**, *16*, 2148, doi:10.3390/s16122148.
26. Turco, A.; Pennetta, A.; Caroli, A.; Mazzotta, E.; Monteduro, A.G.; Primiceri, E.; de Benedetto, G.; Malitesta, C. Easy Fabrication of Mussel Inspired Coated Foam and Its Optimization for the Facile Removal of Copper from Aqueous Solutions. *J Colloid Interface Sci* **2019**, *552*, 401–411, doi:10.1016/j.jcis.2019.05.059.
27. González-Rivera, J.; Iglio, R.; Barillaro, G.; Duce, C.; Tinè, M.R. Structural and Thermoanalytical Characterization of 3D Porous PDMS Foam Materials: The Effect of Impurities Derived from a Sugar Templating Process. *Polymers (Basel)* **2018**, *10*, 616, doi:10.3390/polym10060616.
28. Xu, B.; Ye, F.; Chen, R.; Luo, X.; Xue, Z.; Li, R.; Chang, G. A Supersensitive Wearable Sensor Constructed with PDMS Porous Foam and Multi-Integrated Conductive Pathways Structure. *Ceram Int* **2023**, *49*, 4641–4649, doi:10.1016/j.ceramint.2022.09.351.
29. Vadalà, M.; Kröll, E.; Küppers, M.; Lupascu, D.C.; Brunstermann, R. Hydrogen Production via Dark Fermentation by Bacteria Colonies on Porous PDMS-Scaffolds. *Int J Hydrogen Energy* **2023**, doi:10.1016/j.ijhydene.2023.03.285.

30. Choi, S.J.; Kwon, T.H.; Im, H.; Moon, D. Il; Baek, D.J.; Seol, M.L.; Duarte, J.P.; Choi, Y.K. A Polydimethylsiloxane (PDMS) Sponge for the Selective Absorption of Oil from Water. *ACS Appl Mater Interfaces* **2011**, *3*, 4552–4556, doi:10.1021/am201352w.
31. Jiang, H.; Zhu, Y.; Zhao, G.; Tian, A.; Li, H.; Li, J.; Zhao, S.; Zhang, G.; Gao, A.; Cui, J.; et al. Preparation and Optimisation of Conductive PDMS Composite Foams with Absorption-Dominated Electromagnetic Interference Shielding Performance via Silvered Aramid Microfibers. *Eur Polym J* **2023**, *191*, 112029, doi:10.1016/j.eurpolymj.2023.112029.
32. Sosnin, I.M.; Vlassov, S.; Akimov, E.G.; Agenkov, V.I.; Dorogin, L.M. Hydrophilic Polydimethylsiloxane-Based Sponges for Dewatering Applications. *Mater Lett* **2020**, *263*, 127278, doi:10.1016/j.matlet.2019.127278.
33. Wang, L.; Fu, J.; Jiang, X.; Li, D. Efficient Extraction Approach Based on Polydimethylsiloxane/ZIF-Derived Carbons Sponge Followed by GC–MS for the Determination of Volatile Compounds in Cumin. *Food Chem* **2023**, *405*, doi:10.1016/j.foodchem.2022.134775.
34. Maia, R.; Sousa, P.; Pinto, V.; Soares, D.; Lima, R.; Minas, G.; Rodrigues, R.O. PDMS Porous Microneedles Used as Engineered Tool in Advanced Microfluidic Devices and Their Proof-of-Concept for Biomarker Detection. *Chemical Engineering Journal* **2024**, *485*, doi:10.1016/j.cej.2024.149725.
35. Tebboth, M.; Jiang, Q.; Kogelbauer, A.; Bismarck, A. Inflatable Elastomeric Macroporous Polymers Synthesised from Medium Internal Phase Emulsion Templates. *ACS Appl Mater Interfaces* **2015**, *7*, 19243–19250, doi:10.1021/acsami.5b05123.
36. Chen, S.; Zhuo, B.; Guo, X. Large Area One-Step Facile Processing of Microstructured Elastomeric Dielectric Film for High Sensitivity and Durable Sensing over Wide Pressure Range. *ACS Appl Mater Interfaces* **2016**, *8*, 20364–20370, doi:10.1021/acsami.6b05177.
37. Turco, A.; Primiceri, E.; Frigione, M.; Maruccio, G.; Malitesta, C. An Innovative, Fast and Facile Soft-Template Approach for the Fabrication of Porous PDMS for Oil-Water Separation. *J Mater Chem A Mater* **2017**, *5*, 23785–23793, doi:10.1039/c7ta06840a.
38. Kovalenko, A.; Zimny, K.; Mascaro, B.; Brunet, T.; Mondain-Monval, O. Tailoring of the Porous Structure of Soft Emulsion-Templated Polymer Materials. *Soft Matter* **2016**, *12*, 5154–5163, doi:10.1039/c6sm00461j.
39. Timusk, M.; Nigol, I.A.; Vlassov, S.; Oras, S.; Kangur, T.; Linarts, A.; Šutka, A. Low-Density PDMS Foams by Controlled Destabilization of Thixotropic Emulsions. *J Colloid Interface Sci* **2022**, *626*, 265–275, doi:10.1016/j.jcis.2022.06.150.
40. Zhang, L.; Zhang, Y.; Chen, P.; Du, W.; Feng, X.; Liu, B.F. Paraffin Oil Based Soft-Template Approach to Fabricate Reusable Porous PDMS Sponge for Effective Oil/Water Separation. *Langmuir* **2019**, *35*, 11123–11131, doi:10.1021/acs.langmuir.9b01861.
41. Dong, Y.; Wang, L.; Xia, N.; Yang, Z.; Zhang, C.; Pan, C.; Jin, D.; Zhang, J.; Majidi, C.; Zhang, L. Untethered Small-Scale Magnetic Soft Robot with Programmable Magnetization and Integrated Multifunctional Modules. *Sci Adv* **2022**, *8*, 8932, doi:10.1126/sciadv.abn8932.
42. Kwak, Y.; Kang, Y.; Park, W.; Jo, E.; Kim, J. Fabrication of Fine-Pored Polydimethylsiloxane Using an Isopropyl Alcohol and Water Mixture for Adjustable Mechanical, Optical, and Thermal Properties. *RSC Adv* **2021**, *11*, 18061–18067, doi:10.1039/d1ra02466c.
43. Juchniewicz, M.; Stadnik, D.; Biesiada, K.; Olszyna, A.; Chudy, M.; Brzózka, Z.; Dybko, A. Porous Crosslinked PDMS-Microchannels Coatings. *Sens Actuators B Chem* **2007**, *126*, 68–72, doi:10.1016/j.snb.2006.10.041.
44. Alatawi, L.; Abdullah, A.H.; Jamil, S.N.A.Md.; Yunus, R. A Facile and Green Synthesis of Hydrophobic Polydimethylsiloxane Foam for Benzene, Toluene, and Xylene Removal. *Separations* **2023**, *10*, 377, doi:10.3390/separations10070377.
45. Xu, J.; Zhu, S.; Liu, P.; Gao, W.; Li, J.; Mo, L. Adsorption of Cu(II) Ions in Aqueous Solution by Aminated Lignin from Enzymatic Hydrolysis Residues. *RSC Adv* **2017**, *7*, 44751–44758, doi:10.1039/c7ra06693g.
46. Ayawei, N.; Ebelegi, A.N.; Wankasi, D. Modelling and Interpretation of Adsorption Isotherms. *J Chem* 2017, *2017*.
47. Mamaghanifar, Z.; Heydarinasab, A.; Ghadi, A.; Binaeian, E. BTX Removal from Aqueous Solution Using Copper- and Nickel-Modified Zeolite 4A: Kinetic, Thermodynamic, and Equilibrium Studies. *Water Conservation Science and Engineering* **2020**, *5*, 1–13, doi:10.1007/s41101-019-00079-0.
48. Jodeh, S.; Ahmad, R.; Suleiman, M.; Radi, S.; Emran, K.M.; Salghi, R.; Warad, I.; Hadda, T. Ben Kinetics, Thermodynamics and Adsorption of Btx Removal from Aqueous Solution via Date-Palm Pits Carbonization Using SPME/GC-MS. *Journal of Materials and Environmental Science* **2015**, *6*, 2853–2870.
49. Carvalho, M.N.; da Motta, M.; Benachour, M.; Sales, D.C.S.; Abreu, C.A.M. Evaluation of BTEX and Phenol Removal from Aqueous Solution by Multi-Solute Adsorption onto Smectite Organoclay. *J Hazard Mater* **2012**, *239–240*, 95–101, doi:10.1016/j.jhazmat.2012.07.057.
50. Sahoo, T.R.; Prelot, B. Adsorption Processes for the Removal of Contaminants from Wastewater: The Perspective Role of Nanomaterials and Nanotechnology. In *Nanomaterials for the Detection and Removal of Wastewater Pollutants*; Elsevier, 2020; pp. 161–222 ISBN 9780128184899.
51. Hristovski, K.D.; Markovski, J. Engineering Metal (Hydr)Oxide Sorbents for Removal of Arsenate and Similar Weak-Acid Oxyanion Contaminants: A Critical Review with Emphasis on Factors Governing Sorption Processes. *Science of the Total Environment* **2017**, *598*, 258–271, doi:10.1016/j.scitotenv.2017.04.108.
52. Tan, K.L.; Hameed, B.H. Insight into the Adsorption Kinetics Models for the Removal of Contaminants from Aqueous Solutions. *J Taiwan Inst Chem Eng* **2017**, *74*, 25–48, doi:10.1016/j.jtice.2017.01.024.

53. Aivalioti, M.; Pothoulaki, D.; Papoulias, P.; Gidarakos, E. Removal of BTEX, MTBE and TAME from Aqueous Solutions by Adsorption onto Raw and Thermally Treated Lignite. *J Hazard Mater* **2012**, *207–208*, 136–146, doi:10.1016/j.jhazmat.2011.04.084.
54. Si, P.; Wang, J.; Zhao, C.; Xu, H.; Yang, K.; Wang, W. Preparation and Morphology Control of Three-Dimensional Interconnected Microporous PDMS for Oil Sorption. *Polym Adv Technol* **2015**, *26*, 1091–1096, doi:10.1002/pat.3538.
55. Colosi, C.; Costantini, M.; Barbetta, A.; Pecci, R.; Bedini, R.; Dentini, M. Morphological Comparison of PVA Scaffolds Obtained by Gas Foaming and Microfluidic Foaming Techniques. *Langmuir* **2013**, *29*, 82–91, doi:10.1021/la303788z.
56. Masihi, S.; Panahi, M.; Maddipatla, D.; Hanson, A.J.; Bose, A.K.; Hajian, S.; Palaniappan, V.; Narakathu, B.B.; Bazuin, B.J.; Atashbar, M.Z. Highly Sensitive Porous PDMS-Based Capacitive Pressure Sensors Fabricated on Fabric Platform for Wearable Applications. *ACS Sens* **2021**, *6*, 938–949, doi:10.1021/acssensors.0c02122.
57. Wan Hamad, W.N.F.; Teh, P.L.; Yeoh, C.K. Effect of Acetic Acid as Catalyst on the Properties of Epoxy Foam. *Polymer - Plastics Technology and Engineering* **2013**, *52*, 754–760, doi:10.1080/03602559.2012.762375.
58. Labouriau, A.; Cox, J.D.; Schoonover, J.R.; Patterson, B.M.; Havrilla, G.J.; Stephens, T.; Taylor, D. Mössbauer, NMR and ATR-FTIR Spectroscopic Investigation of Degradation in RTV Siloxane Foams. *Polym Degrad Stab* **2007**, *92*, 414–424, doi:10.1016/j.polymdegradstab.2006.11.017.
59. Grissom, T.G.; Sharp, C.H.; Usov, P.M.; Troya, D.; Morris, A.J.; Morris, J.R. Benzene, Toluene, and Xylene Transport through UiO-66: Diffusion Rates, Energetics, and the Role of Hydrogen Bonding. *Journal of Physical Chemistry C* **2018**, *122*, 16060–16069, doi:10.1021/acs.jpcc.8b03356.
60. Hou, L.; Li, X.; Xie, D.; Wang, H. Effects of BTEX on the Removal of Acetone in a Coaxial Non-Thermal Plasma Reactor: Role Analysis of the Methyl Group. *Molecules* **2018**, *23*, doi:10.3390/molecules23040890.
61. Klomkliang, N.; Do, D.D.; Nicholson, D. Affinity and Packing of Benzene, Toluene, and p-Xylene Adsorption on a Graphitic Surface and in Pores. *Ind Eng Chem Res* **2012**, *51*, 5320–5329, doi:10.1021/ie300121p.
62. Li, Z.; Zhang, Y.; Niu, J.; Tao, T.; Zhao, R.; Li, Z.; Ye, C.; Li, D.; Fan, L. A Porous Aromatic Framework as a Versatile Fiber Coating for Solid-Phase Microextraction of Polar and Nonpolar Aromatic Organic Compounds. *Microchimica Acta* **2019**, *186*, 1–8, doi:10.1007/s00604-019-3669-1.
63. Guelli Ulson De Souza, S.M.; Da Luz, A.D.; Da Silva, A.; Ulson De Souza, A.A. Removal of Mono- and Multicomponent BTX Compounds from Effluents Using Activated Carbon from Coconut Shell as the Adsorbent. *Ind Eng Chem Res* **2012**, *51*, 6461–6469, doi:10.1021/ie2026772.
64. Mamaghanifar, Z.; Heydarinasab, A.; Ghadi, A.; Binaeian, E. BTX Removal from Aqueous Solution Using Copper- and Nickel-Modified Zeolite 4A: Kinetic, Thermodynamic, and Equilibrium Studies. *Water Conservation Science and Engineering* **2020**, *5*, 1–13, doi:10.1007/s41101-019-00079-0.
65. Bandura, L.; Kołodyńska, D.; Franus, W. Adsorption of BTX from Aqueous Solutions by Na-P1 Zeolite Obtained from Fly Ash. *Process Safety and Environmental Protection* **2017**, *109*, 214–223, doi:10.1016/j.psep.2017.03.036.
66. Jang, Y.; Bang, J.; Seon, Y.S.; You, D.W.; Oh, J.S.; Jung, K.W. Carbon Nanotube Sponges as an Enrichment Material for Aromatic Volatile Organic Compounds. *J Chromatogr A* **2020**, *1617*, doi:10.1016/j.chroma.2019.460840.
67. Guo, M.; Liang, H.; Luo, Z.; Chen, Q.; Wei, W. Study on Melt-Blown Processing, Web Structure of Polypropylene Nonwovens and Its BTX Adsorption. *Fibers and Polymers* **2016**, *17*, 257–265, doi:10.1007/s12221-016-5592-y.
68. Mustafa, S.K.; Al-Aoh, H.A.; Bani-Atta, S.A.; Alrawashdeh, L.R.; Aljohani, M.M.H.; Alsharif, M.A.; Darwish, A.A.A.; Al-Shehri, H.S.; Ahmad, M.A.; Al-Tweher, J.N.; et al. Enhance the Adsorption Behavior of Methylene Blue from Wastewater by Using Zncl2 Modified Neem (Azadirachta Indica) Leaves Powder. *Desalination Water Treat* **2021**, *209*, 367–378, doi:10.5004/dwt.2021.26494.